The International Journal of Advanced Manufacturing Technology (2022) 120:4963–4976
https://doi.org/10.1007/s00170-022-09004-7

ORIGINAL ARTICLE

Bonding integrity of hybrid 18Ni300-17-4 PH steel using the laser powder bed fusion process for the fabrication of plastic injection mould inserts

Yuk Lun Simon Chan[1,2] · Olaf Diegel[1,2] · Xun Xu[2]

Received: 19 November 2021 / Accepted: 1 March 2022 / Published online: 23 March 2022

Abstract
Laser powder bed fusion (LPBF) is a metal additive manufacturing (AM) process for fabricating high-performance functional parts and tools in various metallic alloys, such as titanium, aluminium and tool steels. One specific AM application is fabricating conformal cooling channels (CCC) in plastic injection moulding tool inserts to improve cooling efficiency. This article reports the development of a novel hybrid powder-wrought alloy steel combination intended for injection mould inserts use. In this investigation, cylindrical parts made of 18Ni300 steel powder and wrought 17-4 PH steel were additively fabricated using a hybrid-build LPBF AM technique, followed by various post-build heat treatments. Standard mechanical and microstructural techniques were employed to examine the bonded powder-substrate interface. Microstructure analysis revealed defect-free, fully dense, homogenous powder-substrate fusion across a 280-µm-thick region. Tensile tests confirmed strong powder-substrate bonding due to solid solution strengthening within the region. All tensile fractures were ductile under all heat treatment conditions and occurred about 8 mm from the interface, at the side where the materials were of lower strength. The hybrid-built parts exhibited an ultimate tensile strength of 1009–1329 MPa, with 16.1–17.4% elongation at fracture. Hardness values on the AM-deposited and substrate sides were 31–55 HRC and 32–43 HRC, respectively. A direct post-build 490 °C/1 h age-hardening treatment achieved the best combination of hardness, tensile strength and ductility. The overall result demonstrates that hybrid-built powder 18Ni300-wrought 17-4 PH steel can be a material choice for manufacturing durable and high-performance injection mould inserts for high-volume production.

Keywords Additive manufacturing · Hybrid-build · Laser powder bed fusion · Maraging 300 steel · 17-4 PH steel

1 Introduction

Laser powder bed fusion (LPBF) is a metal additive manufacturing (AM) process utilising high intensified laser energy to selectively fuse fine metal powder particles layer upon layer within regions of a powder bed [1]. With modern metal AM systems, the process can fabricate fully dense high-performance functional parts and tools of high complexity in various metallic alloys such as titanium, stainless steel, aluminium, and tool steels. One specific application is the fabrication of conformal cooling channels (CCC) for injection mould inserts to improve cooling efficiency [2–4]. Despite its functional benefit, this new technology is still not widely adopted in the mould-making industry as the processing speeds are slow and metal AM systems are expensive.

A recent attempt by Chan et al. [5] using a hybrid-build LPBF AM technique to fabricate aluminium mould inserts with CCC attained a substantial reduction in processing time, making it an attractive alternative method to the mould-making industry. However, before this technique can be implemented in actual industrial applications, it is critical to choose the right powder-substrate material combination and understand their fusion bonding behaviour.

✉ Yuk Lun Simon Chan
ycha723@aucklanduni.ac.nz

Olaf Diegel
olaf.diegel@auckland.ac.nz

Xun Xu
x.xu@auckland.ac.nz

[1] Creative Design and Additive Manufacturing Lab, The University of Auckland, Auckland, New Zealand

[2] Department of Mechanical and Mechatronics Engineering, The University of Auckland, Auckland, New Zealand

Several studies have been successfully carried out on fusing similar and dissimilar metals using different manufacturing processes for various applications. These studies involved: bonding of powder Inconel 718 with solid 316 stainless steel using a direct energy deposition process for oil exploration equipment [6], fabrication of aluminium-magnesium bimetallic composites using a lost foam casting solid-liquid compound process for automotive and aerospace parts [7], bonding of powder AlSi10Mg with solid aluminium alloys using the LPBF process for mould inserts [8]. Additional techniques such as surface coating and ultrasonic vibration have also been employed to enhance the mechanical strength of the interface [9, 10].

The findings from these studies proved the practicability of the bonding concept for industrial applications. Nonetheless, as tool steel is the preferred material type for constructing high-volume high-performance plastic injection moulds [11], further investigation is needed on whether a similarly successful outcome could apply to tool steels.

Recently, a few investigations have been conducted on the bonding of 18Ni300 maraging steel powder with various wrought tool steels using the LPBF process. Early work on fracture behaviour of hybrid-built 18Ni300-H13 steel revealed that peak hardness/tensile strength could be achieved with a special age-hardening treatment targeting the H13 substrate [12]. However, tensile fracture occurred at the bonded interface. It was later suggested that the failure was caused by a combination of chemical and microstructural inhomogeneity, compounded by increased porosity at the 18Ni300-H13 interface [13]. Another study on fracture toughness of hybrid-built 18Ni300-H13 and 18Ni300-420 tool steels also found a crack growth path along the interfacial boundary, indicating a brittle mechanics fracture resulting from build defects [14]. Therefore, even though H13 and 420 are widely used tool steels for manufacturing high-grade plastic injection moulds, their suitability as the substrate for combining powder 18Ni300 maraging steel in the hybrid-build approach, as demonstrated by the studies mentioned above, is questionable.

These shortcomings could be addressed by choosing wrought precipitation-hardenable steels, such as 17-4 PH steel, as the substrate material for bonding. As both maraging 300 and 17-4 PH are precipitation-hardenable steels, it is believed that they would be compatible with the laser fusion and post-build heat treatment processes. Nevertheless, no study has yet focused on this powder-substrate combination. Hence, 17-4 PH steel was chosen as the substrate material in this study. If successful, this unique steel combination could be a material choice for manufacturing durable and high-performance injection mould inserts using the LPBF hybrid-build technique. Therefore, results from this line of inquiry will have significant implications for industry practice.

2 Background

2.1 18Ni300 maraging steel

Maraging steels are a unique class of low-carbon, high-nickel steels that acquire their strength from the precipitation of intermetallic alloy elements. They are renowned for their superior strength, high toughness, good machinability, good weldability and dimensional stability through age-hardening. One particular grade, 18Ni300, is commonly used as tool steel for extrusion dies, plastic injection moulds, aluminium and zinc die casting moulds, and hot pressing dies [15]. Due to its popularity in industries, LPBF built 18Ni300 maraging steel has been widely studied for its suitability in metal AM applications since the early 2010s.

Early investigation in the processing of this material by Yasa et al. revealed that, at a specific energy density threshold, near-fully dense parts with mechanical properties comparable to the wrought counterpart could be produced by applying laser re-melting after every layer [16]. However, this came at the cost of longer build time. They also found that while an increase in laser scanning speed and layer thickness affected the macrohardness due to higher porosity, their effect on the microhardness was insignificant. Equipped with more advanced LPBF systems, researchers recently carried out in-depth studies on other influential process parameters. One study reported that an XY scanning strategy could reduce the anisotropy and surface roughness of the AM built parts, resulting in high-quality products with homogeneous mechanical properties [17]. Another study found that processed with a thicker powder layer of 50 µm could reduce energy consumption and production time with only a slight reduction in strength and ductility [18].

As mentioned earlier, the strength and hardness of wrought maraging steels can be enhanced via an age-hardening process. This heat treatment process allows the formation of a uniform distribution of fine nickel-rich intermetallic precipitates to strengthen the martensitic matrix [19]. Hence, it is imperative to examine and understand the behaviour of aged LPBF-built 18Ni300 steel parts. Among various age-hardening conditions, a combination of ageing temperature at 480 °C for 5 h was found to give an ultra-high-strength of about 2200 MPa and high hardness of about 650 HV (58 HRC) [16]. However, when compared with the as-built condition, ductility dropped substantially by nearly 90 to 1.6% after ageing. A later investigation by Tan et al. [20] revealed that ductility could be increased to about 3.3% by heat-treating the parts at 490 °C for 6 h. Moreover, a two-step solution annealing (840 °C/1 h) and age hardening (490 °C/6 h) technique could further increase the ductility to 5.6% with only a slight drop in ultimate tensile strength.

When considering using LPBF-built maraging steel as mould inert material, understanding its post-build machinability is essential as the AM fabricated part will require post-build machining to achieve the final dimensions and shape. It was known that the anisotropic nature and grain size of materials fabricated by the LPBF process could affect the cutting forces [21]. A recent study by Bai et al. [22] revealed that as-built and solution-annealed maraging steel parts have better machinability than the age-hardened ones. The cutting force and tool wear decreased by almost 50% in comparison. As a result, different cutting parameters are needed for age-hardened surfaces.

2.2 17-4 PH steel

17-4 PH steel is a low-carbon, high-chromium martensitic stainless steel grade. Due to its good corrosion resistance and excellent mechanical properties, 17-4 PH steel is widely used as structural materials for chemical and power plants, aerospace parts and mechanical engineering components [23]. Hence, it could be well-suited as the base structure/substrate for hybrid-building of injection mould inserts. Like 18Ni300 maraging steel, 17-4 PH steel can be aged or precipitation-hardened to achieve ultra-high strength and high hardness [24–26]. Hence, additively built parts with 18Ni300 powder-wrought 17-4 PH steel can be post-processed using similar heat treatment procedures.

2.3 Methodology

In this study, a novel hybrid-alloy steel material was developed for injection moulding inserts. This investigation is an ongoing research project on hybrid-built hybrid-metal by the authors. Hence, the same experimental methodology applied in the previous hybrid-aluminium study [8] was also employed here in this hybrid-alloy steel study.

Powder 18Ni300 steel was additively deposited onto pre-machined round wrought 17-4 PH blanks using the LPBF process. The mechanical and metallurgical properties of the bonded interface of as-built and heat-treated hybrid-built samples were investigated. Tensile tests were conducted to determine the rupture position and the strength of the hybrid-built specimens. Stand-alone LPBF-built 18Ni300 and wrought 17-4 PH samples were also used as a baseline in the tensile test for comparison. Optical microscopy (OM), scanning electron microscopy (SEM), and energy-dispersive X-ray spectroscopy (EDS) techniques were employed to examine the 18Ni300-17-4 PH interface and fracture surfaces. Microhardness tests were also performed to identify the hardness change across the region. A possible application using this manufacturing technique was also proposed.

3 Experimental procedure

3.1 Materials

The materials chosen for this investigation were 18Ni300 maraging steel powder, supplied by EOS GmbH under the trade name MS1, and wrought 17-4 PH stainless steel, supplied in solution-treated condition (condition A) by BGH Edelstahl Freital GmbH. Table 1 shows the chemical composition of both materials as stated in the test certificates. The gas-atomised MS1 steel powder particles, as stated in the certificate [27], were predominantly spherical with diameter ranges between 20 and 54 µm (Fig. 1). The wrought 17-4 PH steel was supplied as 19.05 mm round stock.

3.2 Processing

3.2.1 Design of hybrid-build samples

Two types of hybrid-build samples were designed for tensile tests (TT) and microstructure analysis (MA), as shown in Fig. 2. All substrate blanks were prepared by turning from the 19-mm-diameter stock bar. After the LPBF process, specimens for examination (shaded area in Fig. 2) were obtained by conventional CNC turning and milling.

3.2.2 Fabrication

Eight hybrid-built samples, four for tensile test and four for microstructure analysis, were fabricated in one single build on an EOS M290 metal LPBF machine. The EOS M290 is a mid-size metal AM machine with a building volume of 250 × 250 × 325 mm and a 400-W 100-µm-diameter Yb fibre laser. All substrate blanks were mounted onto the build plate with M6 cap screws under 14 Nm of tightening torque. In addition, four stand-alone 18Ni300 tensile samples, Ø10 × 45 mm in size, were fabricated vertically from a separate setup for

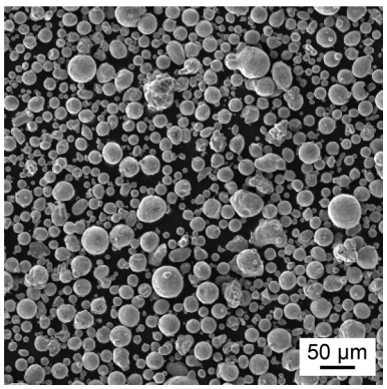

Fig. 1 SEM micrograph of MS1 powder (excerpted from [27])

Table 1 Chemical composition of the materials used in this study (wt.%)

	C	Si	Mn	P	S	Cr	Mo	Ni	Ti	Cu	Nb	Co	Al	Ta	Fe
18Ni300	0.01	0.09	0.05	0.01	0.01	0.13	4.57	17.27	0.68	0.02	na	8.53	0.09	na	Bal.
17-4 PH	0.05	0.37	0.63	0.02	na	15.6	0.13	4.22	na	3.21	0.25	0.03	na	0.01	Bal.

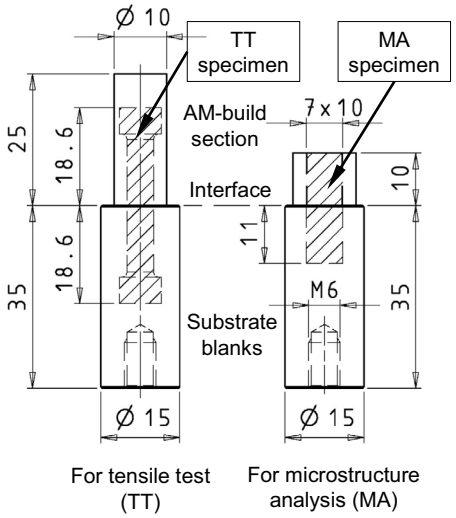

Fig. 2 Design of the hybrid-build samples

baseline strength comparisons. In both builds, the build plate's temperature was set to 40 °C, and the build chamber was made inert with nitrogen gas to maintain the oxygen concentration at 1.3%. As recommended by EOS, optimised LPBF process parameters for MS1, as listed in Table 2, were used for the two builds. Additionally, the first three layers of powder were set to be scanned twice or re-melted by the laser to ensure defect-free bonding. Figure 3 shows the two types of fabricated hybrid 18Ni300-17-4 PH samples.

3.2.3 Post-build heat treatments

Three different types of samples, as-built/as-supplied, solution-annealed, and age-hardened in four groups, were examined in this study. Three samples from each group were heat-treated, one solution-annealed and two age-hardened. Before heat treatments, all samples were pre-machined, with minimum material stock left for final turning, milling and surface grinding (Fig. 4). The heat treatment conditions used were designated as:

- HT0 - as-built/as-supplied
- HT1 - solution annealing, 940 °C/2 h/air cooling
- HT2 - age-hardening, 490 °C/1 h/air cooling
- HT3 - age-hardening, 490 °C/6 h/air cooling

Both HT1 and HT3 are conditions specified by EOS for MS1 maraging steel for industry practice, whereas HT2 was set in this study for evaluation. Table 3 lists all the set heat treatment conditions for this study. All heat treatments were carried out in a laboratory-type Thermo Fisher F30430 muffle furnace. All heat-treated samples were air-cooled outside the furnace.

Table 2 LPBF process parameters for EOS MS1

Laser power	Hatch spacing	Scan velocity	Layer thickness	Scan pattern
285 W	0.11 mm	960 mm/s	0.04 mm	Stripes, 10 mm wide, 47° rotation angle

3.3 Characterisation

3.3.1 Tensile test

Standardised tensile tests were performed according to BS EN ISO 6892-1 standard [28] with Instron 1185 tensile testing machines to evaluate the strength of the hybrid-built, stand-alone AM-built and wrought samples. All twelve tensile test specimens were produced by CNC turning, with dimensions as specified in the standard. The four hybrid-built samples were machined with the bonded interface positioned at the middle of the specimen (Fig. 5).

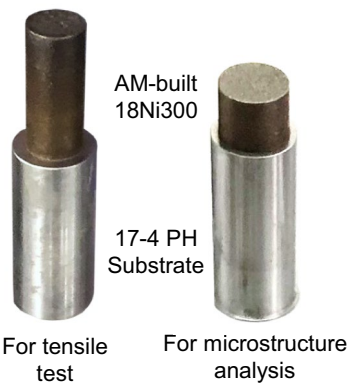

Fig. 3 Fabricated 18Ni300-17-4 PH samples

Table 3 Set heat treatment conditions for this study

	For tensile test	For microstructure analysis
Hybrid 18Ni300-17-4 PH	HT0, HT1, HT2, HT3	HT0, HT1, HT2, HT3
Stand-alone 18Ni300	HT0, HT1, HT2, HT3	Not applicable
Wrought 17-4 PH	HT0, HT1, HT2, HT3	Not applicable

All tests were executed at room temperature until failure occurred. The parameters used for the tensile tests were:

- Gauge length: 25 mm
- Gauge diameter: 5 mm
- Testing rate: 0.375 mm/min

3.3.2 Microstructure analysis

The microstructural behaviour at the interface of the hybrid-built steel specimens is of prime interest in this study. Standard optical microscopy (OM), scanning electron microscopy (SEM), and energy-dispersive X-ray spectroscopy (EDS) techniques were employed to examine the interface. All four specimens were cast in a phenolic mounting block and then polished, lapped, and etched with 3% Nital (3% HNO3-97% Ethanol) etchant (Fig. 6).

Before etching, the relative density or porosity of the specimens, an area of 3.6 mm × 2.2 mm with the interface roughly in the middle, was measured by the image processing software ImageJ. Micrographs of the microstructure were obtained with an Olympus BX60M optical microscope and an FEI Quanta scanning electrode microscope. The powder-substrate interface thickness of the hybrid-built non-heat-treated specimen was evaluated using EDS line scanning with the scanning electrode microscope.

Fig. 4 Pre-machined and heat-treated 18Ni300-17-4 PH samples

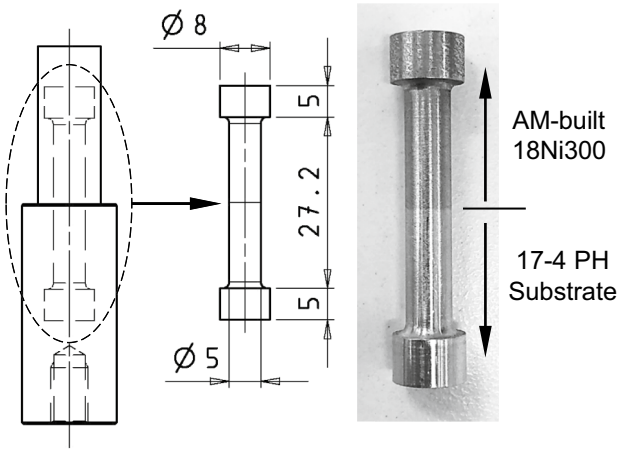

Fig. 5 Hybrid-built tensile test specimen

3.3.3 Hardness measurement

The microhardness line profile (HV0.2) across the interface of the four MA specimens was measured with a Struers DuraScan 50 microhardness tester. The scan length was 1 mm, with the interface being approximately in the middle of the scan. Twenty-one hardness measurements were recorded at 50-µm intervals. For discussion purposes, all measured values were converted to the equivalent in Rockwell "C" scale (HRC).

4 Results and discussions

The microstructure and mechanical properties of additively manufactured 18Ni300 and conventional wrought 17-4 PH steel have been well studied and documented in the past two decades. Therefore, the following discussions are focused primarily on the interfacial region between the powder and substrate materials.

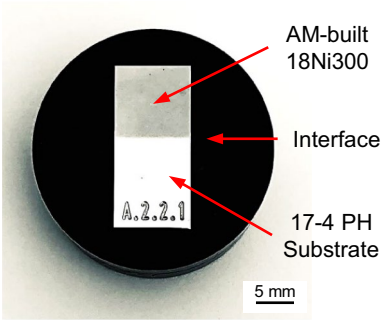

Fig. 6 Mounted specimen for microstructure analysis

4.1 Microstructure of the 18Ni300-17-4 PH interface

4.1.1 Microstructural observation

OM and SEM micrographs of the as-built and heat-treated specimens are presented in Figs. 7 and 8, respectively. No visible cracks or defects were detected, and the calculated relative density through porosity measurement was 0.999 or 99.9%. Hence, it is fair to consider the four hybrid-built samples as fully dense. Figure 7a depicts the OM micrographs of the two materials, which correspond to the AM-build direction: AM-deposited 18Ni300 at the top, 17-4 PH substrate at the bottom. It also shows a region (bound by the two red lines) where the transition of the substrate to powder material took place. As evaluated from the EDS line scan (Fig. 9), the thickness of this region in which the transfer of the four major alloying elements, Cr, Ni, Co and Mo, occurred between the powder and substrate material was approximately 280 µm. A similar thickness of bonded interface was also reported in a recent study on LPBF-processed hybrid Corrax-PH13-8Mo steel [29].

As shown in Figs. 7a and 8a, d and g, the morphology of the AM-deposited side corresponded with observations reported in past studies on additively manufactured 18Ni300 steel. In Fig. 7a, prominent fish-scale morphology of overlapping melt pools was identified at the AM-deposited side of the as-built specimen, typical of LPBF fabricated maraging 300 steel [16]. By contrast, the fish-scale pattern disappeared entirely in the HT1 or solution-treated specimen (Fig. 8a). Instead, the cell-type structure was replaced by a homogenised large lath martensite microstructure, a similar observation reported by Song et al. [30]. In comparison, while still present, the fish-scale morphology was barely visible in the direct HT2 and HT3 age-treated specimens (Fig. 8d and g). Moreover, a smaller lath-like structure and small intermetallic precipitates were noticed in these two specimens (Fig. 8e and h), bearing a close resemblance to those found on a specimen age-treated with 450 °C for 6h without solution annealing [31].

By definition, the interface is the region where fusion bonding of 18Ni300 powder and wrought 17-4 PH substrate occurred. The morphology in this narrow region, as expected, was a blend of the AM-deposited 18Ni300 and wrought 17-4 PH resulting from the interaction of the laser with the powder and substrate materials. As seen in Fig. 7a, the fish-scale morphology of the 18Ni300 in the upper region was less distinct, gradually becoming less noticeable towards the 17-4 PH substrate side, and eventually disappeared beyond the middle of the region.

A subtle trace of the 18Ni300 melt pool boundaries was still visible at the upper interfacial boundary in the as-built and age-hardened specimens (Figs. 7a and 8d and g). This

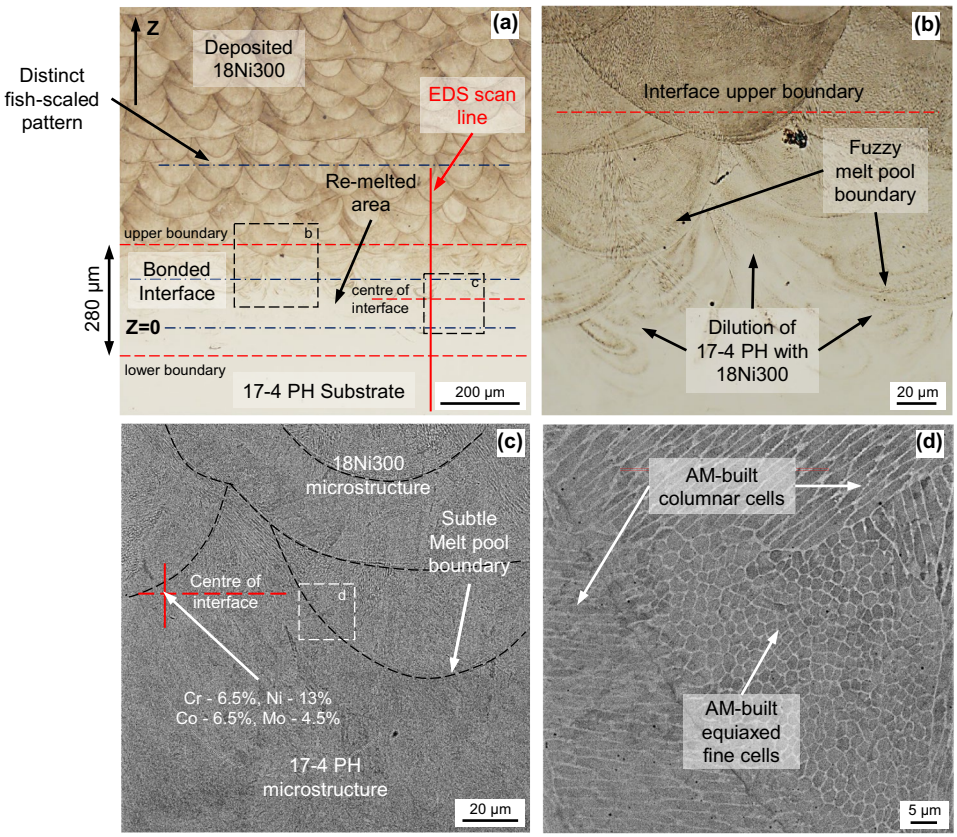

Fig. 7 Micrographs of the as-built 18Ni300-17-4 PH specimen: (**a**-**b**) OM, (**c**-**d**) SEM

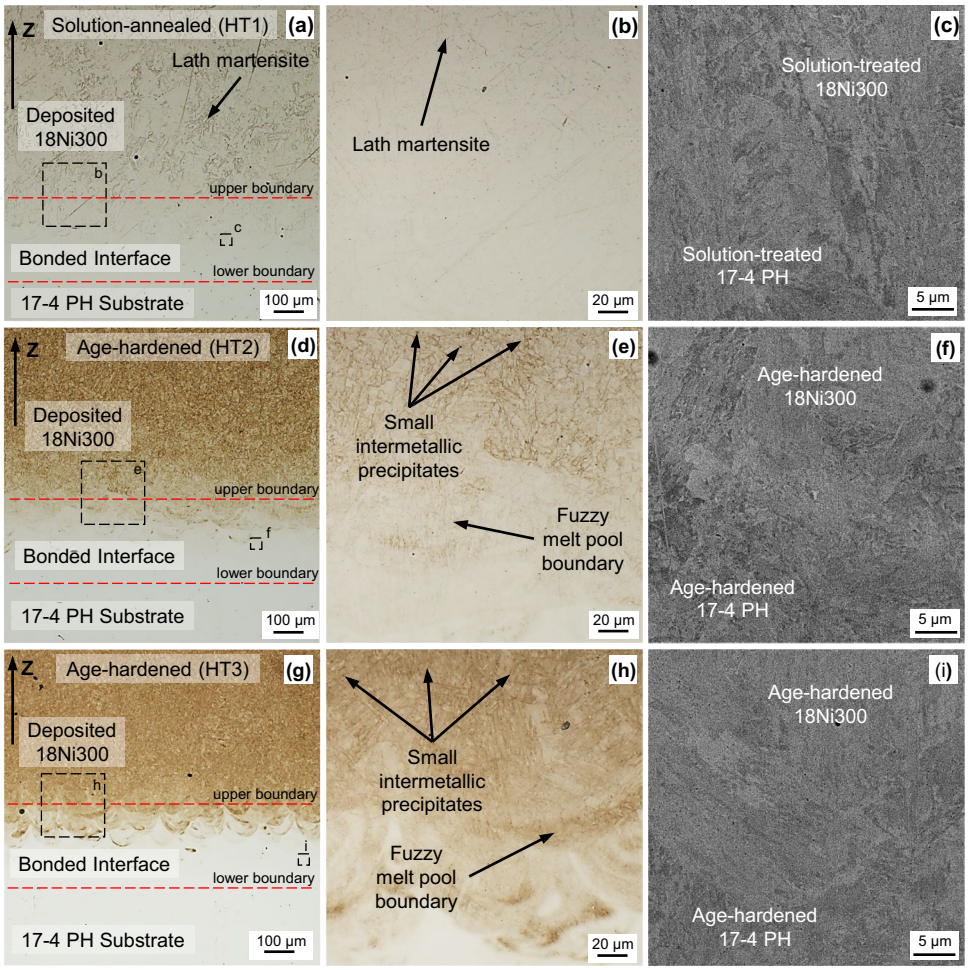

Fig. 8 OM and SEM micrographs of the heat-treated18Ni300-17-4 PH specimens: (**a**–**c**) solution annealed with HT1, (**d**–**f**) age-hardened with HT2, (**g**–**i**) age-hardened with HT3

resulted from the partial melting and mixing of the 17-4 PH substrate with the powder material. High magnification OM images revealed that the original fish-scale morphology became fuzzy (Figs. 7b and 8e and h). Around the middle section of the interface, the microstructure of both 18Ni300 and 17-4 PH can be seen. In the as-built specimen, a mixture of AM-built 18Ni300 columnar dendritic and fine equiaxed cells together with wrought solution-treated 17-4 PH structure was detected (Fig. 7c and d). Similarly, well-blended microstructures of heat-treated AM-built 18Ni300 and 17-4 PH were also found in high magnification SEM micrographs (Fig. 8c, f and i). According to the EDS line scan (Fig. 9), the weight percentage of the four major alloying elements, Cr, Ni, Co and Mo, were roughly averaged out around the centre of the interface (Fig. 7c). This homogenous mixing characteristic of the two materials is further discussed in the following subsection.

4.1.2 Characteristic of the bonded interface

At the start of the AM-build process (z=0), the partial melting of the 17-4 PH substrate and mixing its alloying elements with the melted 18Ni300 powder created a dilution effect. Hence, the chemical composition of the melt pool consisted of a mixture of both materials. Dilution of alloying elements has also been reported in hybrid-built 18Ni300-CMnAlNb [32] and 18Ni300-H13 [13] steel parts. EDS line scan performed in this study revealed a homogenous mixing or dilution of the 18Ni300 and 17-4 PH material.

In Fig. 9, the rates of change of the four alloying elements were slightly faster during the first quarter of the interface region before they became steady towards the other end, indicating that the dilution of 17-4 PH with 18Ni300 happened quickly during the start of the AM-build. It is believed to result from the fusion process designed for this study. The AM-build process was set to have the first three layers (120 µm) of 18Ni300 powder scanned twice or re-melted. The re-melting process allowed the alloying elements of the 18Ni300 to penetrate below the substrate top surface twice, facilitating homogenous mixing across the initial 120 µm thickness. As the build carried on, the transfer of the alloying elements happened more gradually. Overall, the dilution formed a solid solution rich in alloying elements from the 18Ni300 (Ni, Co and Mo) and 17-4 PH (Cr). Consequently,

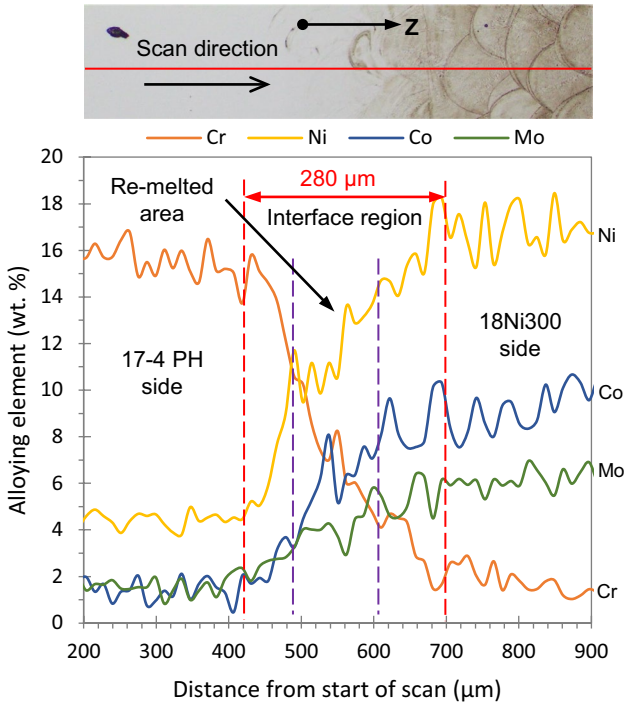

Fig. 9 EDS line scan across the interface of the as-built 18Ni300-17-4PH specimen

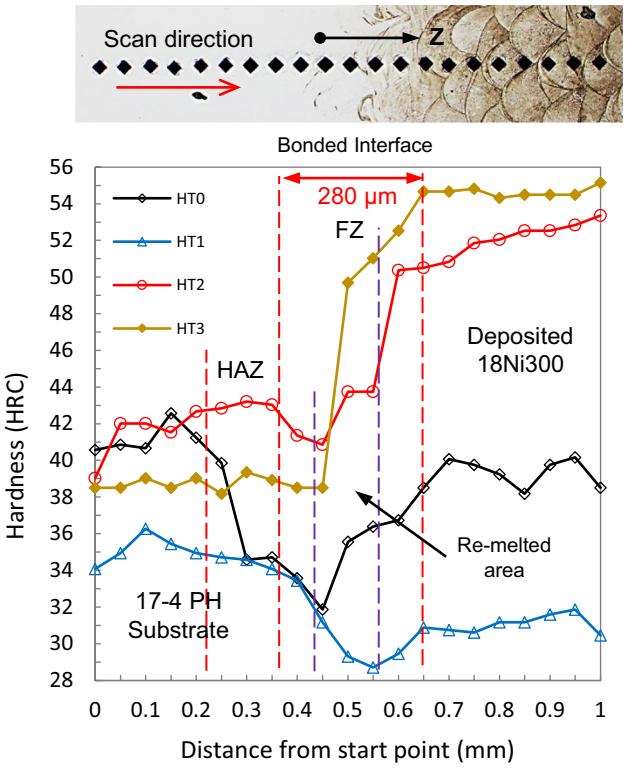

Fig. 10 Microhardness profiles of the hybrid-built samples with different heat treatment conditions

a higher strength interfacial bond can be expected from this solid solution strengthening mechanism [33]. The effect of this interfacial microstructural change on the mechanical properties of the hybrid-built samples is discussed in the next section.

4.2 Mechanical properties

In the die and mould manufacturing industry, tensile strength, ductility and hardness are considered the three key mechanical properties of tool steels for fabricating strong and durable mould components. Hence, these three key properties of the hybrid-built 18Ni300-17-4 PH parts are discussed in the following subsections to establish the applicability of the hybrid-build concept.

4.2.1 Hardness

The results of the microhardness line profile measurements of the four hybrid-built samples are shown in Fig. 10. The interfacial boundaries established from the EDS line scan and the re-melting area are also referenced. Overall, the effect of different heat treatment conditions on the hardness of the two materials was as expected; hardness was lower with solution annealing but was higher with age-hardening. The same hardness change pattern was also reported in LPBF built maraging 300 steel using the same heat treatment methodology [20].

On the AM-deposited 18Ni300 side, the hardness value obtained on the as-built or HT0 sample was about 39 HRC. In comparison, the values on the samples heat-treated with HT1, HT2 and HT3 were about 31, 53 and 55 HRC, respectively. It can be seen that the hardness dropped by 8 HRC hardness points or about 20% through HT1 treatment. This widely documented softening was the result of the homogenised microstructural change in the material after the solution treatment (ST) process. It was also noticed that further softening could occur with a higher set ST temperature.

In this study, the ST condition was set at 940 °C/2 h, the latest recommendation by the powder manufacturer. In comparison, Song et al. [30] used a lower setting of 840 °C for the same duration and reported a 6 HRC hardness point drop. The extra softening obtained in this study could benefit pre-hardening machining operations. In contrast to solution annealing, the two age-hardened samples exhibited a relatively big jump in hardness, 14 HRC points or 36% with HT2 and 16 HRC points or 41% with HT3. It is worth noting that an additional 5 h for HT3 over HT2 resulted only in an additional 5% gain in hardness. This shorter duration makes the HT2 or 490 °C/1 h age-hardening treatment a preferable method for injection mould application.

On the 17-4 PH substrate side, although the material followed the same pattern of hardness change from treatment HT1 to HT3, the recorded hardness on the HT3 sample was lower than that of the as-supplied one. A possible explanation would be the incompatibility of the heat treatment setting used on the 17-4 PH material, as the heat treatment conditions used in this study were primarily designed for 18Ni300 steel. According to a previous study [34], a relatively high hardness of about 49 HRC was recorded with a combined solution-age treatment condition set at 1040 °C/0.5 h followed by 510 °C/1 h. Nevertheless, the 43 HRC hardness obtained on the substrate side of the HT2 sample in this study would still be suitable for mould application.

Around the interface, the hardness profile of the as-built sample followed a down-up pattern across the region from the substrate to the AM-deposited side. The hardness value dropped from about 41 HRC starting at about 1.5 mm from the interface to 32 HRC inside the region. It then climbed back up to about 39 HRC towards the 18Ni300 side of the interface before levelling off. The softening behaviour on the 17-4 PH side of the interface was due to the local tempering of the 17-4 PH material. The interfacial region and its substrate neighbour can be considered equivalent to fusion zone (FZ) and heat-affected zones (HAZ) in the case of conventional laser welding. As the fusion started in the build process, the temperature in the HAZ was high enough to trigger coarsening and dissolution of precipitates of the 17-4 PH [35]. However, the intermetallic precipitates were evenly dispersed with ageing treatments, resulting in a more uniform microhardness profile, as seen in Fig. 10. The steady climb of hardness within the fusion zone is evidence of the solid solution strengthening effect created by the dilution of 18Ni300 with 17-4 PH, as discussed in Section 4.1.2. Moreover, the increase in hardness of the 17-4 PH substrate within the re-melted area is also evidence of surface hardening through the laser scanning process [36].

4.2.2 Fracture behaviour

All 12 specimens, four of hybrid-built 18Ni300-17-4 PH, four of stand-alone AM-built 18Ni300, and four of wrought 17-4 PH, were pulled to rupture under uniaxial tensile tests. The fracture behaviour of the hybrid-built samples is of particular interest in this study.

Figure 11 shows the photos of the four ruptured hybrid-built specimens, illustrating the rupture points relative to the interface line. As can be seen from the photos, the rupture point occurred about 8 mm from the interface line on either the AM-built 18Ni300 side for the as-built and solution-annealed specimens or the 17-4 PH substrate side for the two age-hardened specimens. As expected, no fracture occurred at the interface line, confirming a robust bonding between the powder and substrate material. The intact of the fusion

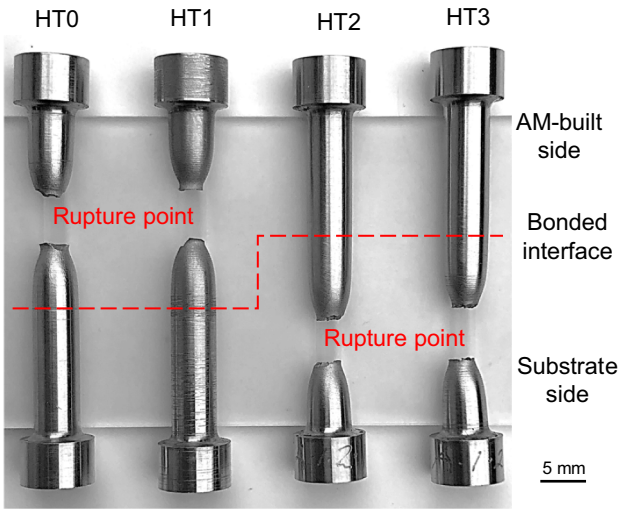

Fig. 11 Hybrid-built 18Ni300-17-4 PH ruptured specimens

joints is further proof of the solid solution strengthening effect on the interface, as discussed in Section 4.1.2. Furthermore, all four specimens ruptured after substantial necking, suggesting ductile fractures.

SEM fractographs of the four hybrid-built specimens are depicted in Fig. 12. The fracture surface morphology of the HT0 (Fig. 12a and e) and HT1 (Fig. 12b and f) specimens are very similar to those presented in previous 18Ni300 steel studies [20, 30], in which a large number of dimples of various sizes and depth were formed, indicating a typical transgranular ductile fracture. Similarly, the fractured 17-4 PH surfaces on HT2 (Fig. 12c and g) and HT3 (Fig.12d and h) consist of large transgranular dimples and highly nonuniform smaller ones which are characteristic fracture morphology of aged 17-4 PH steel [37].

These fracture behaviours are of significance as they proved the reliability of this manufacturing technique. This provides confidence in using this hybrid-build hybrid-alloy steel material for manufacturing high-performance injection mould inserts.

4.2.3 Mechanical strength

The recorded values of the 0.2% proof or yield strength (YS), ultimate tensile strength (UTS) and elongation at fracture (EF) were listed in Table 4. The results for the hybrid-built samples were depicted graphically in Fig. 13. For discussion purposes, the strength and ductility of the three groups of samples under the four different heat treatment conditions were shown in Fig. 14a and b.

Among the four hybrid-built samples, the one with the HT2 treatment exhibited the highest YS, UTS and EF of 1220 MPa, 1329 MPa and 17.4%, respectively. The second highest strength was recorded on the as-built or HT0

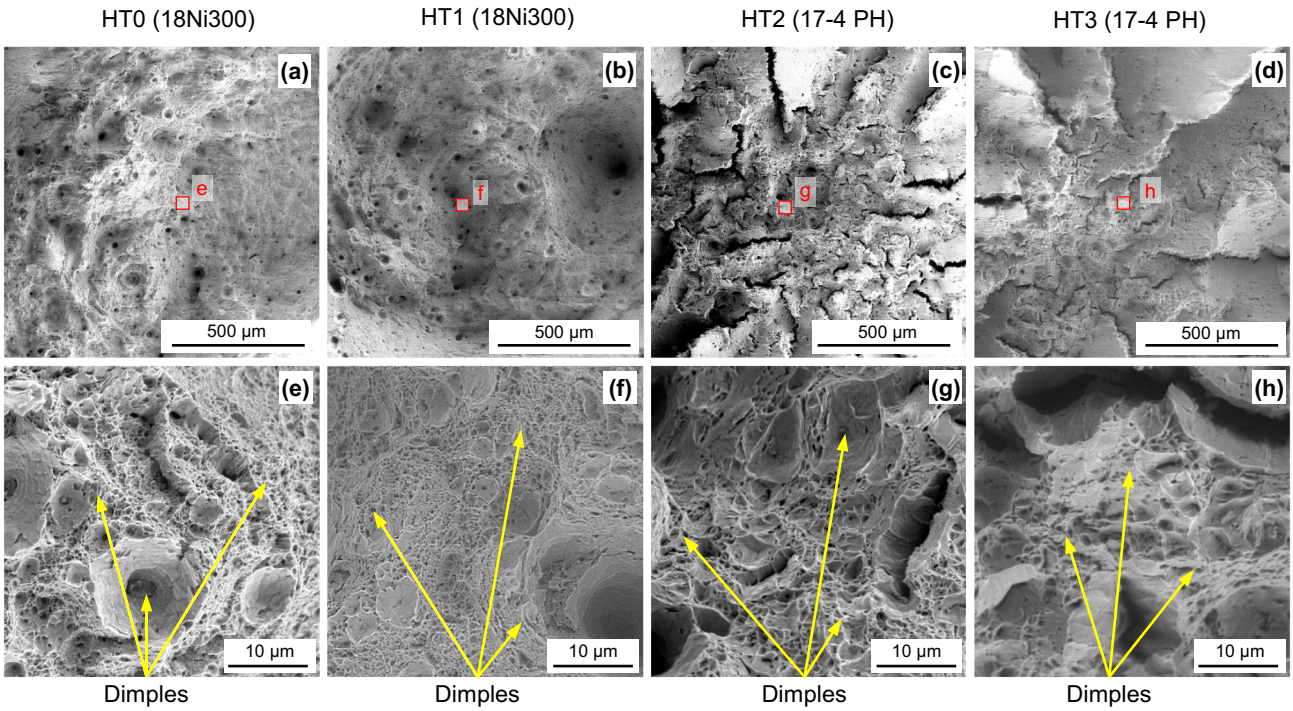

Fig. 12 SEM fractographs of the tensile test specimens under the four different heat treatment conditions, (**a**, **e**) HT0, (**b**, **f**) HT1, (**c**, **g**) HT2, (**d**, **h**) HT2

sample (UTS = 1200 MPa), followed by HT3 (UTS = 1159 MPa) and HT1 (UTS = 1009 MPa). Compared with the as-built sample, an increase of about 10% on average in strength was noticed. The strengthening effect on 18Ni300 and 17-4 PH steel resulting from ageing treatment was well documented [16, 24]. As expected, the solution annealing treatment reduced the strength of the HT1 sample substantially, from 1200 to 1009 MPa, or about 16%. Overall, the ductility of these four samples could be considered high, with EF values ranging from 16 to 17.5%. Long necking, or elongation from UTS to failure, of about 10% on the four samples is also proof of high ductility. These results were comparable to the findings reported in a recent hybrid-steel study [32]. When comparing the

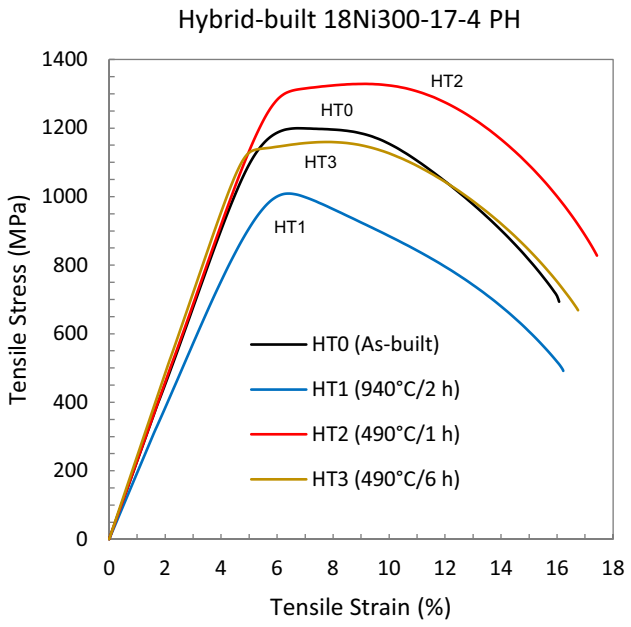

Fig. 13 Tensile stress-strain curves of the hybrid-built specimens with different heat treatments

Table 4 Comparison of mechanical strength

Sample	YS (MPa)	UTS (MPa)	EF (%)
Hybrid 18Ni300-17-4 PH (HT0)	1130	1200	16.1
Hybrid 18Ni300-17-4 PH (HT1)	930	1009	16.3
Hybrid 18Ni300-17-4 PH (HT2)	1220	1329	17.4
Hybrid 18Ni300-17-4 PH (HT3)	1130	1159	16.8
Stand-alone 18Ni300 (HT0)	1040	1093	13.2
Stand-alone 18Ni300 (HT1)	890	996	16.1
Stand-alone 18Ni300 (HT2)	1770	1847	12.6
Stand-alone 18Ni300 (HT3)	1940	1966	11.4
Wrought 17-4 PH (HT0)	1110	1233	16.7
Wrought 17-4 PH (HT1)	940	1098	17.1
Wrought 17-4 PH (HT2)	1310	1372	18.7
Wrought 17-4 PH (HT3)	1240	1285	18.8

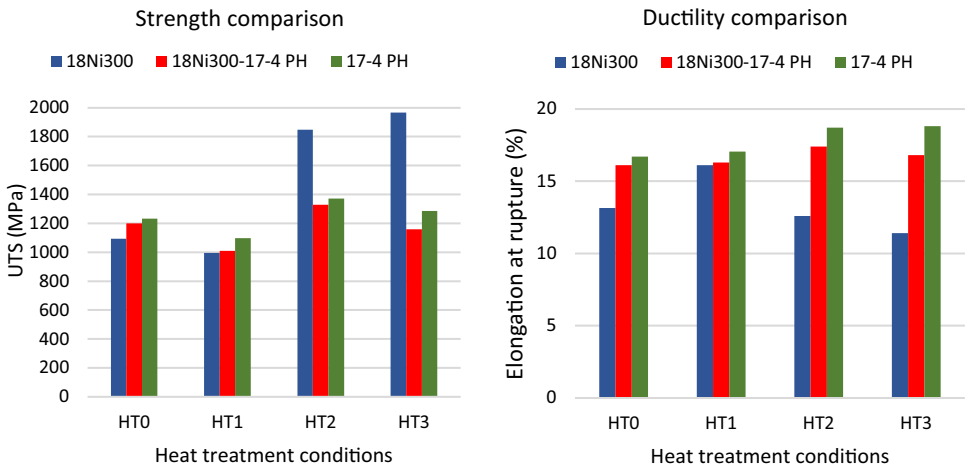

Fig. 14 Bar charts comparing the difference between hybrid-built and stand-alone samples under the four different heat treatment conditions, **a**) in strength, **b**) in ductility

HT0 with the HT3 sample, the 6-h ageing treatment had no strengthening effect on the HT3 sample as a whole part. Instead, it lowered its strength by about 4% and increased its ductility by about the same amount.

In order to better understand the mechanical behaviours of these hybrid-steel parts, a comparison between the hybrid-built, stand-alone AM-built 18Ni300 and wrought 17-4 PH samples is needed. In Fig. 14a, it can be seen that the difference in UTS between 18Ni300 and 17-4 PH as a stand-alone material was comparatively large when subjected to the HT2 and HT3 ageing treatments. The ductility comparison also noticed the same but opposite trend (Fig. 14b). The stand-alone HT2 and HT3 treated 18Ni300 samples had the two highest strengths (UTS = 1847 and 1966 MPa) but the two lowest ductilities (EF = 12.6 and 11.4%). It would explain why tensile failure with ductile necking occurred on the 17-4 PH substrate side or the weaker side of the hybrid-built HT2 and HT3 samples (Fig. 11). Conversely, under the conditions of HT0 and HT1, stand-alone AM-built 18Ni300 samples were not as strong and as ductile as the 17-4 PH counterparts. Consequently, tensile failure occurred on the weaker side, the AM-built 18Ni300 side of these two hybrid-built samples (Fig. 11). From these observations and comparisons, the most suitable condition to acquire a balanced strength-ductility property for hybrid-built 18Ni300-17-4 PH parts as a whole would be to use the post-build HT2 ageing treatment.

In summary, microstructure analysis and mechanical testing revealed fully dense and strong interfacial bonds between the powder and substrate materials, confirming the success of the hybrid-build technique. Furthermore, age-hardened hybrid-built 18Ni300-17-4 PH steel parts possessed high mechanical strength, high hardness and high ductility. The

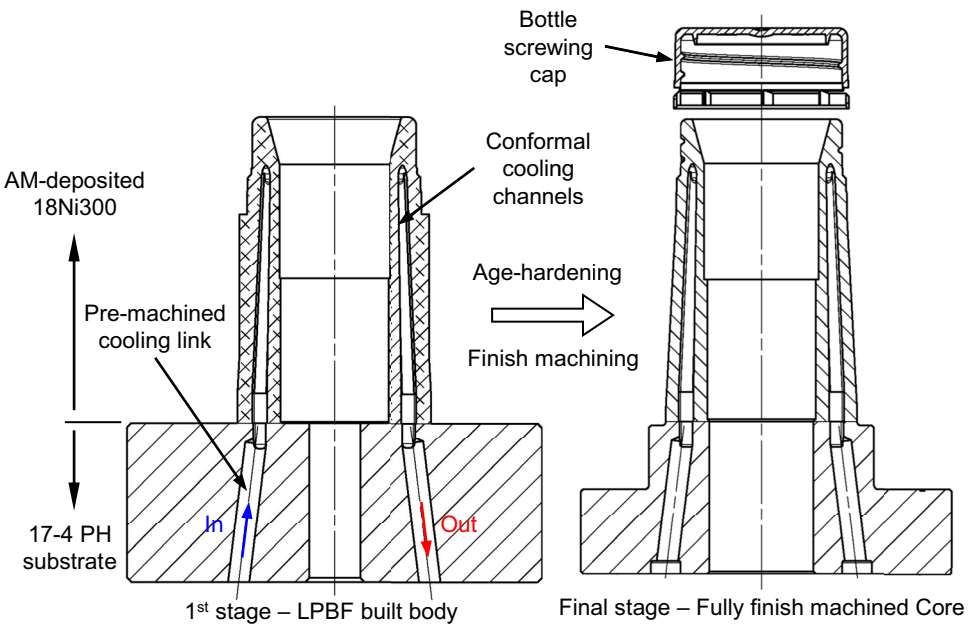

Fig. 15 A proposed hybrid-build design of a core in hybrid-steel with conformal cooling channels

best combination of strength (1329 MPa), hardness (43/53 HRC) and ductility (17.4%) was attained on the sample with the post-build direct 490 °C/1 h ageing treatment.

5 Potential application

The findings from this study open up opportunities for mould designers and mould makers to combine the new metal AM technology with well-established conventional practice. Figure 15 shows an example of how this hybrid-build concept can produce a durable mould insert with high cooling efficiency.

The core, as an insert, is part of the mould that produces a drink bottle screw cap. This design shows how cooling water can get up to the top to cool around the thread via conformal cooling channels (CCC). This portion of the core, including the internal product shape, in 18Ni300 steel, will be additively fabricated on a pre-machined 17-4 PH round blank using the LPBF process. The wrought 17-4 PH portion will form the base of the core insert. The AM-build CCC will link up with the pre-machined cooling holes in the substrate blank to form a complete cooling circuit.

After the LPBF and heat treatment process, the core will be finish-machined to its final shape and details. As a result, an efficiently cooled mould insert with high strength and high hardness is expected. Future detailed investigation on manufacturing costs and mould performance of this proposed design could prove the cost-effectiveness of this LPBF-machined substrate hybrid AM strategy.

6 Conclusion

In this study, hybrid-alloy steel parts were successfully fabricated additively by depositing 18Ni300 steel powder on pre-machined wrought 17-4 PH stainless steel using the LPBF process. Experimental results on mechanical and metallurgical properties of the hybrid-built parts confirmed the practicability of the hybrid-build hybrid-steel manufacturing technique. The key findings from this study can be summarised as follows:

- A bonded interfacial region of approximately 280 µm in thickness was formed between the powder and substrate steel by the LPBF process.
- Microstructure analysis revealed defect-free, fully dense, well-penetrated and well-diluted powder-substrate fusion across the interface. In as-built condition, a mixture of LPBF-built columnar dendritic and fine equiaxed 18Ni300 cells together with wrought solution-treated 17-4 PH structure was detected. After age-hardening, this mixture was well-blended into a homogenous microstructure of 18Ni300 and 17-4 PH, proving a high-integrity fusion bond.
- Parts fabricated using the hybrid-build method exhibit strong powder-to-substrate bonding with ductile tensile failure that occurred well away from the interface on the side of the material with the lower strength. This occurrence confirmed the effect of solution strengthening within the fusion bond.
- The most suitable post-build heat treatment to produce hybrid-built parts of high strength, high hardness and high ductility was the direct 490 °C/1 h method.

In conclusion, additively fabricated powder 18Ni300-wrought 17-4 PH steel can be a good material choice for manufacturing durable and high-performance injection mould inserts using the LPBF hybrid-build AM technique. It could provide a cost-effective alternative for the mould manufacturing industry.

Acknowledgements The authors wish to thank CAMEX 2018 Limited for providing the machinery and labour to prepare the samples.

Author contributions This research will provide a practical solution for combining powder and wrought tool steel for fabricating durable mould insert using the laser powder bed fusion process. Yuk Lun Simon Chan, as a PhD student, undertook the bulk of the hands-on research part of the project, under the supervision of Olaf Diegel and Xun Xu, and the paper was collaboratively written by Simon Chan, Olaf Diegel and Xun Xu.

Funding Open Access funding enabled and organized by CAUL and its Member Institutions.

Availability of data and materials The authors are happy to make all the raw experimental data available to anyone who requests it.

Declarations

Ethics approval This research study does not involve human participants, and is to be used for non-life science journals, hence ethical approval is not applicable.

Consent to participate This research study does not involve human participants, and is to be used for non-life science journals, hence consent to participate is not applicable.

Consent for publication The authors give permission for the publishing of this article.

Conflict of interest The authors declare no competing interests.

References

1. ASTM, ISO (2015) ISO/ASTM 52900:2015(E) Standard terminology for additive manufacturing-General principles-Terminology
2. Berger GR, Zorn D, Friesenbichler W, Bevc F, Bodor CJ (2019) Efficient cooling of hot spots in injection molding. A biomimetic cooling channel versus a heat-conductive mold material and a heat conductive plastics. Polym Eng Sci 59(s2):E180–E188. https://doi.org/10.1002/pen.25024
3. Abbès B, Abbès F, Abdessalam H, Upganlawar A (2019) Finite element cooling simulations of conformal cooling hybrid injection molding tools manufactured by selective laser melting. Int J Adv Manuf Technol 103(5–8):2515–2522. https://doi.org/10.1007/s00170-019-03721-2
4. Mazur M, Brincat P, Leary M, Brandt M (2017) Numerical and experimental evaluation of a conformally cooled H13 steel injection mould manufactured with selective laser melting. Int J Adv Manuf Technol 93(1–4):881–900. https://doi.org/10.1007/s00170-017-0426-7
5. Chan YL, Diegel O, Xu X (2021) A machined substrate hybrid additive manufacturing strategy for injection moulding inserts. Int J Adv Manuf Technol 112:557–588. https://doi.org/10.1007/s00170-020-06366-8
6. Yamazaki T (2016) Development of a hybrid multi-tasking machine tool: Integration of additive manufacturing technology with CNC machining. Procedia CIRP, Elsevier 42:81–86. https://doi.org/10.1016/j.procir.2016.02.193
7. Li G, Jiang W, Yang W, Jiang Z, Guan F, Jiang H, Fan Z (2019) New insights into the characterization and formation of the interface of A356/AZ91D bimetallic composites fabricated by compound casting. Metall Mater Trans A Phys Metall Mater Sci A:1076–1090. https://doi.org/10.1007/s11661-018-5022-4
8. Chan YL, Diegel O, Xu X (2021) Evaluation of bonding integrity of hybrid-built AlSi10Mg-aluminium alloys parts using the powder bed fusion process. Mater Today Proc 46:1277–1282. https://doi.org/10.1016/j.matpr.2021.02.126
9. Li G, Jiang W, Guan F, Zhu J, Zhang Z, Fan Z (2021) Microstructure, mechanical properties and corrosion resistance of A356 aluminum/AZ91D magnesium bimetal prepared by a compound casting combined with a novel Ni-Cu composite interlayer. J Mater Process Technol 288:116874. https://doi.org/10.1016/j.jmatprotec.2020.116874
10. Guan F, Jiang W, Wang J, Li G, Zhang Z, Fan Z (2022) Development of high strength Mg/Al bimetal by a novel ultrasonic vibration aided compound casting process. J Mater Process Technol 300:117441. https://doi.org/10.1016/j.jmatprotec.2021.117441
11. Kazmer DO (2016) Injection mold design engineering, 2nd edn. Hanser Publishers, Munich. https://doi.org/10.3139/9783446434196.fm
12. Cyr E, Asgari H, Shamsdini S, Purdy M, Hosseinkhani K, Mohammadi M (2018) Fracture behaviour of additively manufactured MS1-H13 hybrid hard steels. Mater Lett 212:174–177. https://doi.org/10.1016/j.matlet.2017.10.097
13. Azizi H, Ghiaasiaan R, Prager R, Ghoncheh MH, Samk KA, Lausic A, Byleveld W, Phillion AB (2018) Metallurgical and mechanical assessment of hybrid additively-manufactured maraging tool steels via selective laser melting. Addit Manuf 27:389–397. https://doi.org/10.1016/j.addma.2019.03.025
14. Santos LM, de Jesus J, Ferreira JM, Costa JD, Capela C (2018) Fracture toughness of hybrid components with Selective Laser Melting 18Ni300 steel parts. Appl Sci 8(10). https://doi.org/10.3390/app8101879
15. Böhler (2005) Data sheet - Maraging High Strength Steel
16. Yasa E, Kempen K, Kruth JP, Thijs L, Van Humbeeck J (2010) Microstructure and mechanical properties of maraging steel 300 after selective laser melting. Solid Free Fabr Symp Proc pp 383–396
17. Bhardwaj T, Shukla M (2018) Effect of laser scanning strategies on texture, physical and mechanical properties of laser sintered maraging steel. Mater Sci Eng, A 734:102–109. https://doi.org/10.1016/j.msea.2018.07.089
18. Shamsdini SAR, Shakerin S, Hadadzadeh A, Amirkhiz BS, Mohammadi M (2020) A trade-off between powder layer thickness and mechanical properties in additively manufactured maraging steels. Mater Sci Eng A 776:139041. https://doi.org/10.1016/j.msea.2020.139041
19. Carson C (2014) Heat treating of maraging steels. In: ASM Handbook, Vol. 4D Heat Treat. Irons Steels, vol 4D, ASM International, pp 468–480. https://doi.org/10.31399/asm.hb.v04d.a0005948
20. Tan C, Zhou K, Ma W, Zhang P, Liu M, Kuang T (2017) Microstructural evolution, nanoprecipitation behavior and mechanical properties of selective laser melted high-performance grade 300 maraging steel. Mater Des 134:23–34. https://doi.org/10.1016/j.matdes.2017.08.026
21. Pérez-Ruiz JD, de Lacalle LNL, Urbikain G, Pereira O, Martínez S, Bris J (2021) On the relationship between cutting forces and anisotropy features in the milling of LPBF Inconel 718 for near net shape parts. Int J Mach Tools Manuf 170. https://doi.org/10.1016/j.ijmachtools.2021.103801
22. Bai Y, Zhao C, Yang J, Hong R, Weng C, Wang H (2021) Microstructure and machinability of selective laser melted high-strength maraging steel with heat treatment. J Mater Process Technol 288(2020):116906. https://doi.org/10.1016/j.jmatprotec.2020.11690
23. Böhler (2003) Data sheet 17-4 PH Stainless Steel
24. Yoo WD, Lee JH, Youn KT, Rhyim YM (2006) Study on the microstructure and mechanical properties of 17–4 PH stainless steel depending on heat treatment and aging time. Solid State Phenom 118:15–20. https://doi.org/10.4028/www.scientific.net/SSP.118.15
25. Hsiao C, Chiou C, Yang J (2002) Aging reactions in a 17–4 PH stainless steel. Mater Chem Phys 74(2):134–142. https://doi.org/10.1016/S0254-0584(01)00460-6
26. Murayama M, Katayama Y, Hono K (1999) Microstructural evolution in a 17–4 PH stainless steel after aging at 400 °C. Metall Mater Trans A Phys Metall Mater Sci 30(2):345–353. https://doi.org/10.1007/s11661-999-0323-2
27. EOS (2020) Inspection certificate, EOS Maraging Steel MS1
28. CEN, BSI (2019) BS EN ISO 6892-1: 2019 Metallic materials - Tensile testing Part 1: Methods of test at room temperature
29. Marin F, de Souza AF, Ahrens CH, de Lacalle LNL (2021) A new hybrid process combining machining and selective laser melting to manufacture an advanced concept of conformal cooling channels for plastic injection molds. Int J Adv Manuf Technol 113(5–6):1561–1576. https://doi.org/10.1007/s00170-021-06720-4
30. Song J, Tang Q, Feng Q, Ma S, Setchi R, Liu Y, Han Q, Fan X, Zhang M (2019) Effect of heat treatment on microstructure and mechanical behaviours of 18Ni-300 maraging steel manufactured by selective laser melting. Opt Laser Technol 120:105725. https://doi.org/10.1016/j.optlastec.2019.105725
31. Kim D, Kim T, Ha K, Oak JJ, Jeon JB, Park Y, Lee W (2020) Effect of heat treatment condition on microstructural and mechanical anisotropies of selective laser melted maraging 18Ni-300 steel. Metals (Basel) 10(3). https://doi.org/10.3390/met10030410
32. Kučerová L, Zetková I, Jeníček Š, Burdová K (2020) Hybrid parts produced by deposition of 18Ni300 maraging steel via selective laser

melting on forged and heat treated advanced high strength steel. Addit Manuf 32. https://doi.org/10.1016/j.addma.2020.101108
33. Shakerin S, Hadadzadeh A, Amirkhiz BS, Shamsdini S, Li J, Mohammadi M (2019) Additive manufacturing of maraging steel-H13 bimetals using laser powder bed fusion technique. Addit Manuf 29:100797. https://doi.org/10.1016/j.addma.2019.100797
34. Viswanathan UK, Banerjee S, Krishnan R (1988) Effects of aging on the microstructure of 17-4 PH stainless steel. Mater Sci Eng 104(C):181–189. https://doi.org/10.1016/0025-5416(88)90420-X
35. Bahrami Balajaddeh M, Naffakh-Moosavy H (2019) Pulsed Nd:YAG laser welding of 17-4 PH stainless steel: Microstructure, mechanical properties, and weldability investigation. Opt Laser Technol 119. https://doi.org/10.1016/j.optlastec.2019.105651
36. Martínez S, Lamikiz A, Ukar E, Calleja A, Arrizubieta JA, Lopez de Lacalle LN (2017) Analysis of the regimes in the scanner-based laser hardening process. Opt Lasers Eng 90(2016):72–80. http://dx.doi.org/10.1016/j.optlaseng.2016.10.005
37. Rack HJ, Kalish D (1974) The strength, fracture toughness, and low cycle fatigue behavior of 17–4 PH stainless steel. Met Urgical Trans 5(7):1595–1605. https://doi.org/10.1007/BF02646331